

24. *Relation between the Gravity Anomalies and the
Corresponding Subterranean Mass Distribution. (IV)
Isostasy in the United States of America.*

By Chuji TSUBOI, Tetuiti KANEKO,
Setumi MIYAMURA, and Tokutaro YABASI.

Earthquake Research Institute.

(Read Oct. 18, 1938.—Received March 20, 1939.)

1. The present article deals with the application of Tsuboi's method to the interpretation of gravity anomalies, particularly those that are observed in the United States of America. The "Principal Facts for Gravity Stations in the United States," published serially by the U. S. Coast and Geodetic Survey, is the source from which the materials discussed in this study have been drawn. In this connection, we are very thankful to the Director and all the other members concerned in the gravity work of the said Survey for the prompt publication of their observational results in such convenient form that any interested worker could readily use the data provided for the purpose required.

Since Tsuboi¹⁾ has described elsewhere his methods for interpreting gravity anomalies, together with its various applications, they will not be repeated here. The United States is one of the countries in the world in which the distribution of gravity has been extensively surveyed, which is the reason that it has formed the subject of many studies relating to isostatic conditions of the earth's crust. Although the conclusions arrived at with the aid of the present method differ little from what J. H. Hayford, W. Bowie, and W. Heiskanen have already found by the customary trial and error method, owing to the directness and simplicity of the present method, the same conclusions could be obtained with much less elaborate numerical computations.

2. That area in the United States bounded by latitudes $\varphi=30^{\circ}\text{N}$ and $\varphi=48^{\circ}\text{N}$ and longitudes $\lambda=125^{\circ}\text{W}$ and $\lambda=77^{\circ}\text{W}$, was regarded as a plane rectangle with sides approximately 4000 km \times 2000 km. From

1) C. TSUBOI and T. FUCHIDA, *Bull. Earthq. Res. Inst.*, 15 (1937), 636; 16 (1938), 273.

C. TSUBOI, *ibid.*, 15 (1937), 650; 17 (1939), 351; *Proc. Imp. Acad. Tokyo*, 14 (1938), 170.

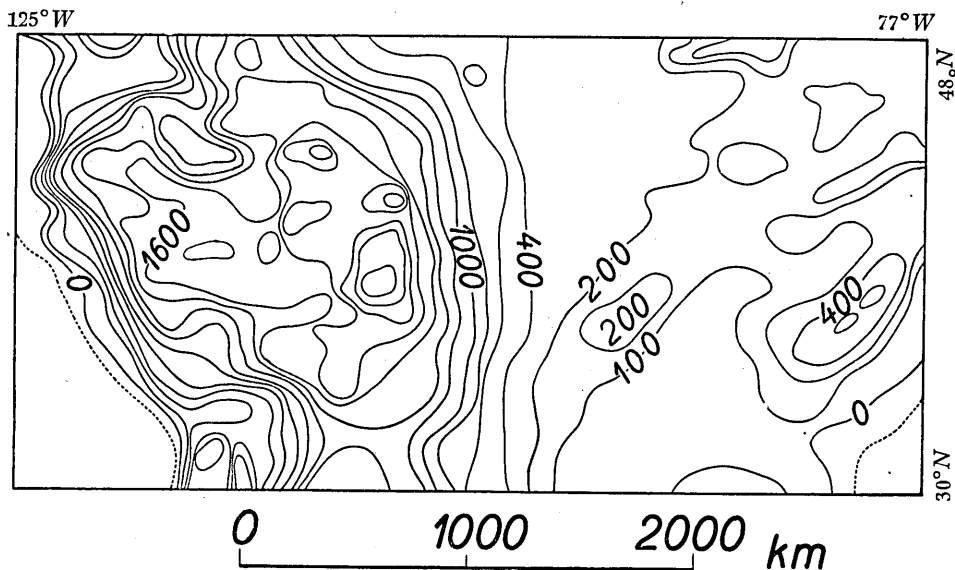


Fig. 1. Height in U. S. A., (m).

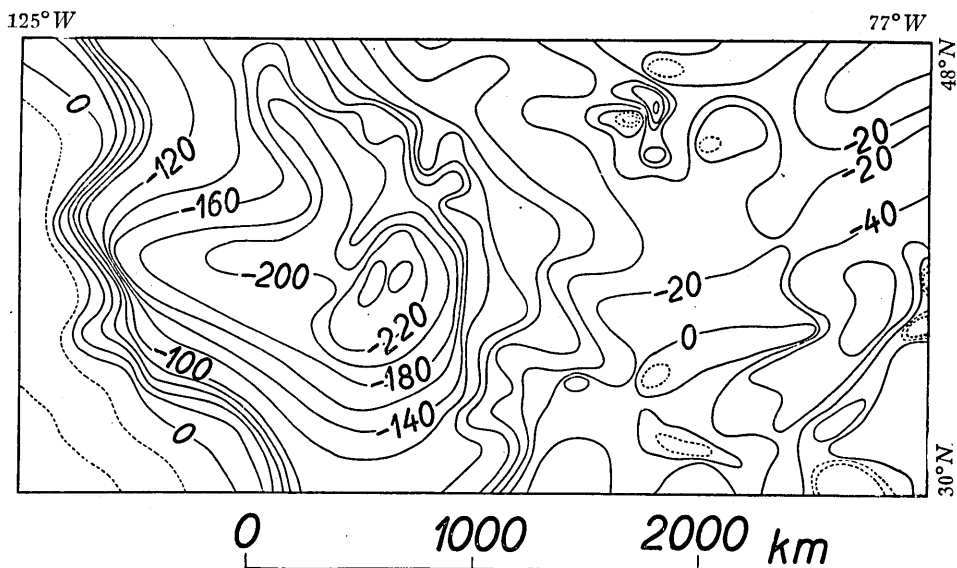


Fig. 2. Bouguer anomaly in U. S. A., (mgal).

the fact that the gravity anomaly that is observed at a point on the earth's surface is mainly determined by the anomalous subterranean mass that lies exactly underneath that point, neglect of the earth's curvature in subsequent calculations does not seem to affect seriously the conclusions. The contour lines for the height H and the Bouguer gravity anomaly $\Delta g''$ in the area are shown in Figs. 1 and 2.

The whole area was divided into $36 \times 36 = 1296$ small rectangles by lines equally spaced and parallel to the sides EW and NS, which will hereinafter be referred to as the x - and y -directions. The heights and the Bouguer anomalies at the 1296 points of intersection of the series of parallel lines were read off by means of interpolations. Both quantities, H and $\Delta g''_o$, each with these 1296 readings, were then analysed into double Fourier series like

$$H(xy) = \sum_0^{18} \sum_0^{18} H_{mn} \cos mx \cos ny,$$

$$\Delta g''_o(xy) = \sum_0^{18} \sum_0^{18} B_{mn} \cos mx \cos ny,$$

taking the distances of 4000 km and 2000 km to be 2π in the x - and y -directions respectively. The double Fourier coefficients H_{mn} and B_{mn} , of which there are 1296 for each, are shown in Tables I and II.

The constant terms H_{oo} and B_{oo} are respectively

$$H_{oo} = 601 \text{ m}$$

$$B_{oo} = -70.9 \text{ mgal.}$$

If isostasy holds in this area, then it must be

$$-2\pi k^2 \rho H_{oo} = B_{oo},$$

where ρ is the density of the crustal material. From this relation, we get

$$\rho = 2.82$$

which is quite a reasonable value. In 712 (55%) out of the whole 1296 pairs of H_{mn} and B_{mn} , they (H_{mn} and B_{mn}) have opposite algebraic signs. As previously explained, that H_{mn} and the corresponding B_{mn} shall have opposite signs is one of the requirements of isostasy. Although 712 slightly exceeds in value those of the remaining 584 pairs in which H_{mn} and B_{mn} have same signs, on the whole, pairs with opposite signs do not seem to predominate. Since, however, the order of the harmonics is a measure of the horizontal extent of the topography, and since we know already that isostasy holds only with topographies of which the horizontal extent exceeds a certain limit, from physical considerations, there is no doubt that the predominance depends on the order m and n .

In order to ascertain this eventual relation, Fig. 3 was constructed. In this figure, a small square that is determined by a certain

Table I a. $H_{m,n}$ in m. (cos-cos)

$n \backslash m$	0	1	2	3	4	5	6	7	8	9	10	11	12	13	14	15	16	17	18
0	601	-394	-138	-6	-84	-3	1	2	-6	13	8	-11	4	5	13	14	6	8	3
1	-237	29	28	70	84	-16	-8	-48	-4	26	7	8	2	-11	8	-2	-2	-3	0
2	-6	24	-27	-26	37	47	-18	3	0	15	27	-8	-21	-9	-4	2	-8	1	-3
3	17	43	9	6	-12	-40	-6	-5	-16	9	18	20	5	5	9	-3	-8	4	2
4	11	20	4	7	-14	-21	7	-7	11	-2	2	3	-10	-7	2	-1	2	2	-1
5	2	10	13	-3	-21	-5	-5	2	-10	9	2	8	6	8	-5	-2	-5	-1	0
6	11	16	15	-11	-2	5	5	2	11	-17	5	-3	1	-8	-8	-5	5	-4	2
7	1	28	-15	14	10	-23	-5	21	16	-9	-10	3	-7	9	-4	-7	-3	1	2
8	1	13	-7	2	8	-20	5	-5	-1	1	2	4	6	0	2	-5	-2	-4	2
9	5	13	-4	4	14	-2	-7	3	1	-1	-7	-5	1	2	-5	-2	1	1	4
10	2	26	-10	2	21	-10	-15	2	8	-1	-2	5	-3	1	-3	-1	-4	-2	-1
11	14	6	-5	8	2	-11	-2	-7	7	-5	-4	-4	5	5	0	-4	-3	-2	3
12	12	18	-6	-4	16	-7	-1	-7	5	-6	2	-4	-1	-5	-2	-7	5	-4	3
13	5	18	-2	-6	4	-9	-1	-1	10	-1	-2	-2	4	3	-1	-5	-3	-2	2
14	5	16	-2	-2	7	0	-11	4	0	-1	-5	1	1	-2	-2	2	3	5	0
15	6	14	0	-5	2	-5	-3	6	5	-5	-2	3	2	3	1	-5	-5	-1	2
16	10	15	2	0	5	-6	-6	-4	4	-7	-1	-7	3	-5	0	-3	2	2	2
17	11	13	-4	-1	5	2	-8	2	-2	0	0	-1	1	-4	-2	2	-1	2	-2
18	5	3	2	-1	4	-1	-2	1	3	-3	2	-4	4	-2	1	-4	0	0	1

Table I c. H_{mn} in m. (sin-cos)

$n \backslash m$	0	1	2	3	4	5	6	7	8	9	10	11	12	13	14	15	16	17	18
0		611	-267	43	-86	-28	-16	-19	-11	-31	1	-11	-8	-10	-8	0	4	-2	
1		-246	22	-34	99	51	50	30	-36	5	1	1	9	-1	-5	2	1	-4	
2		3	34	-59	-63	0	15	-25	5	-14	18	21	6	-3	-10	-1	-2	2	
3		10	24	-18	21	9	6	8	18	-19	-15	2	6	2	2	10	-1	-4	
4		27	15	9	8	-10	-2	1	-14	-2	-7	4	3	-4	-6	-5	-2	1	
5		-8	1	2	-14	3	-8	-2	-12	2	5	2	5	9	8	-2	-2	-2	
6		10	22	-3	-13	-8	5	-11	14	-2	-11	2	4	5	-1	-5	1	-1	
7		11	34	-14	15	9	-14	-2	10	11	-8	-2	-3	2	5	-4	-2	-3	
8		6	21	-12	6	-5	-14	4	-4	4	-2	-1	4	1	3	0	0	-2	
9		8	12	-9	5	13	3	-2	1	5	4	-4	0	4	4	-6	-2	-5	
10		-8	12	-22	1	12	-4	-9	-2	4	-7	6	7	3	4	-4	2	-2	
11		13	8	-4	10	-2	-2	-4	-2	1	-1	-2	-6	5	4	-2	3	-2	
12		2	16	-9	5	6	-1	-4	0	3	-3	-1	-1	0	3	-2	-1	-1	
13		-6	12	-3	6	-2	-2	-1	-2	2	2	-2	-1	0	5	0	0	-2	
14		-5	14	-2	-5	1	-5	-6	0	2	-2	2	5	4	-2	-3	-2	2	
15		-4	14	-1	-5	4	-6	-3	8	-1	2	-2	-2	2	2	2	-3	-5	
16		1	8	-7	-2	2	-5	-7	-1	-1	2	-2	4	4	2	4	2	2	
17		3	10	-1	-4	4	-1	-2	3	-5	-2	-1	2	1	-1	1	-4	2	
18		1	4	-1	-1	0	-2	-3	1	1	1	-2	2	3	2	2	-1	1	

Table II a. B_{mn} in mgal. (cos-cos)

$n \backslash m$	0	1	2	3	4	5	6	7	8	9	10	11	12	13	14	15	16	17	18
0	-70.9	42.1	13.4	3.7	5.3	1.2	-1.2	-2.6	-1.5	-1.1	-1.0	-0.1	-0.3	-1.0	-0.2	-1.1	-0.4	-1.4	0.2
1	28.7	-11.1	-1.7	-9.9	-7.3	1.7	-4.7	0.2	-0.4	2.2	-1.8	-0.4	-1.2	-0.7	-0.5	0.7	-0.8	-0.9	+0.0
2	-4.5	-5.5	-2.7	4.5	-0.1	3.6	2.7	0.5	1.0	-0.4	0.6	-0.6	1.1	0.2	1.8	0.4	1.0	0.9	-0.8
3	-0.3	-2.2	-3.8	-0.4	3.3	-0.3	1.3	2.7	-1.0	-1.1	-0.4	-0.9	-2.9	0.3	-1.6	-0.9	0.1	0.3	-0.4
4	-0.8	-1.9	3.7	2.6	0.2	-1.4	-1.1	-0.7	-2.2	0.3	-0.1	1.4	0.3	0.6	0.7	0.1	0.6	0.4	0.7
5	-0.5	-1.7	1.3	-0.7	-2.1	-0.9	2.4	-0.6	1.6	-0.2	0.4	-0.4	-0.4	0.2	-0.9	0.4	-1.1	-1.5	0.1
6	-0.1	-1.8	2.0	+0.0	0.3	1.8	2.2	0.3	0.1	0.3	-0.3	-0.8	0.6	-0.9	0.2	0.4	0.2	1.2	0.2
7	-1.1	-2.3	0.6	-0.7	-0.0	-0.9	-0.7	-0.6	0.7	0.6	-0.6	0.2	-0.7	-0.3	-0.1	0.1	+0.0	0.3	-0.0
8	-0.8	-1.2	1.4	0.2	0.2	1.5	0.4	0.8	1.0	-0.2	-0.5	0.2	0.8	0.3	0.6	0.1	0.2	-0.1	-0.5
9	-1.2	-1.7	0.2	-0.2	-0.2	1.2	0.3	-0.2	-0.5	-0.8	-0.4	-0.2	-0.2	-0.6	-0.5	-0.3	-0.1	0.3	0.2
10	-0.7	-1.6	0.4	0.1	0.2	0.2	0.3	0.2	0.4	0.0	0.5	-0.4	-0.1	0.3	0.2	0.3	0.4	0.4	0.1
11	-0.6	-1.9	0.9	-0.2	0.5	0.4	0.3	0.1	0.8	-0.1	-0.1	-0.5	-0.1	0.1	-0.6	-0.5	-0.2	-0.2	-0.1
12	-0.8	-1.8	0.4	-0.2	0.2	0.6	-0.2	-0.3	0.1	-0.2	-0.4	0.1	0.5	0.1	-0.2	0.5	0.1	0.1	0.4
13	-1.0	-1.1	0.8	0.3	-0.1	0.2	0.4	-0.3	0.2	0.7	-0.3	-0.1	-0.2	-0.6	0.2	0.2	0.1	-0.2	+0.0
14	-1.1	-1.9	0.2	0.3	0.0	0.2	1.0	0.2	-0.2	0.3	-0.2	-0.1	-0.1	0.2	0.3	-0.2	-0.0	+0.0	-0.2
15	-0.5	-1.3	0.7	0.5	-0.1	-0.0	0.1	-0.0	-0.3	-0.7	+0.0	-0.2	+0.0	-0.2	0.1	-0.2	0.1	0.6	0.5
16	-0.9	-2.4	0.6	0.2	0.0	1.0	+0.0	0.2	-0.1	-0.3	+0.2	-0.4	0.2	-0.4	-0.2	0.1	-0.3	-0.2	+0.0
17	-0.9	-1.1	0.5	0.1	0.2	0.1	0.3	0.1	0.3	0.2	+0.0	0.2	-0.1	-0.1	-0.1	-0.1	+0.0	-0.1	0.1
18	-0.6	-0.7	0.3	+0.0	+0.0	-0.1	0.3	-0.1	-0.1	-0.2	-0.2	-0.0	-0.0	0.1	+0.0	-0.2	-0.1	0.1	0.0

Table II c. B_{mn} in mgal. (sin - cos)

$n \backslash m$	0	1	2	3	4	5	6	7	8	9	10	11	12	13	14	15	16	17	18
0																			
1	-64.0	25.6	2.9	7.3	5.9	6.2	0.9	0.7	0.1	0.8	0.1	0.6	0.6	0.6	1.1	-0.5	-0.3	0.1	
2	25.2	-3.2	2.0	-11.6	-2.1	-0.6	-0.2	-2.0	1.5	-0.3	0.1	-0.7	-0.7	1.3	0.2	-0.2	-0.8	-0.2	
3	-4.4	-11.0	2.5	4.1	0.9	1.7	2.9	1.1	1.9	-1.0	-0.5	-1.2	-1.2	-0.3	-1.4	0.8	0.0	0.3	
4	-1.9	-6.2	0.7	-0.8	-0.2	-1.0	-2.3	2.2	-0.5	0.1	-0.4	0.8	0.8	0.2	-1.1	0.1	-0.3	-0.9	
5	-2.1	0.2	-1.7	1.0	-0.9	0.4	-0.2	0.3	1.1	-0.1	-1.2	-1.2	1.9	-0.5	-0.3	0.2	0.7	-0.1	
6	-1.1	-1.2	-1.3	-1.8	1.9	-0.6	-0.4	0.6	0.5	-0.1	1.0	-0.8	-0.8	0.1	-0.5	-0.9	0.5	-0.5	
7	-2.4	-1.3	-1.4	-0.5	-0.4	0.2	+0.0	1.2	-0.3	1.0	-0.4	-0.4	-0.7	-1.0	-0.3	-0.1	-0.5	-0.3	
8	-0.7	-0.3	0.5	0.9	0.4	0.2	1.0	-0.7	-0.2	0.4	0.3	0.3	0.6	-0.1	0.7	+0.0	-0.3	-0.2	
9	-1.0	-2.6	0.2	0.4	0.4	-0.7	1.6	-1.4	-0.5	-0.1	0.1	0.1	0.3	-0.0	-0.1	+0.0	-0.9	0.4	
10	-1.0	-1.7	0.9	0.6	-0.7	-0.6	0.1	0.4	0.1	0.9	0.2	0.2	0.1	-0.1	-0.4	-0.4	-0.1	-0.1	
11	-0.7	-1.1	0.9	0.3	0.1	0.2	-0.1	0.8	-0.5	0.6	0.3	0.3	-0.1	-0.2	-0.0	-0.4	0.7	-0.6	
12	-1.7	-1.5	0.8	-0.5	0.0	-0.1	0.0	-0.1	-0.1	-0.7	-0.6	0.6	-0.2	-0.1	0.1	-0.2	+0.0	-0.3	
13	-1.9	-0.4	0.1	0.2	0.5	-0.4	0.9	0.6	0.1	0.2	0.4	0.4	0.3	-0.5	0.4	+0.0	-0.6	0.4	
14	-1.7	-0.8	0.7	-0.2	+0.0	-0.2	0.1	-0.0	+0.0	0.1	0.1	0.1	0.2	-0.4	0.1	-0.4	-0.6	-0.1	
15	-1.3	-1.1	0.9	-0.1	0.2	0.3	0.3	-0.4	0.5	-0.2	0.0	0.0	-0.0	0.2	-0.2	+0.0	0.5	-0.2	
16	-1.0	-1.1	1.1	-0.2	-0.4	-0.1	-0.1	0.4	0.1	0.5	-0.1	0.1	0.1	0.0	-0.3	0.5	0.5	-0.1	
17	-1.8	-1.6	0.5	-0.2	0.0	-0.1	0.8	0.3	0.1	0.5	-0.1	-0.1	-0.2	-0.2	-0.5	+0.0	-0.5	-0.1	
18	-1.1	-1.0	0.7	0.2	0.2	-0.4	0.3	-0.2	+0.0	-0.0	0.4	0.4	0.3	-0.3	0.0	-0.5	-0.1	-0.0	
18	-0.7	-0.4	0.1	0.1	+0.0	0.1	0.3	0.2	0.2	+0.0	-0.0	-0.0	-0.1	-0.2	0.1	-0.1	0.2	0.2	

combination of m and n is subdivided into four smaller squares. These small squares will be called the domains of $\sin-\sin$, $\sin-\cos$, $\cos-\sin$, and $\cos-\cos$ respectively, in the order of upper-left, lower-left, upper-right and lower-right. If, in a certain pair of H_{mn} and B_{mn} ,

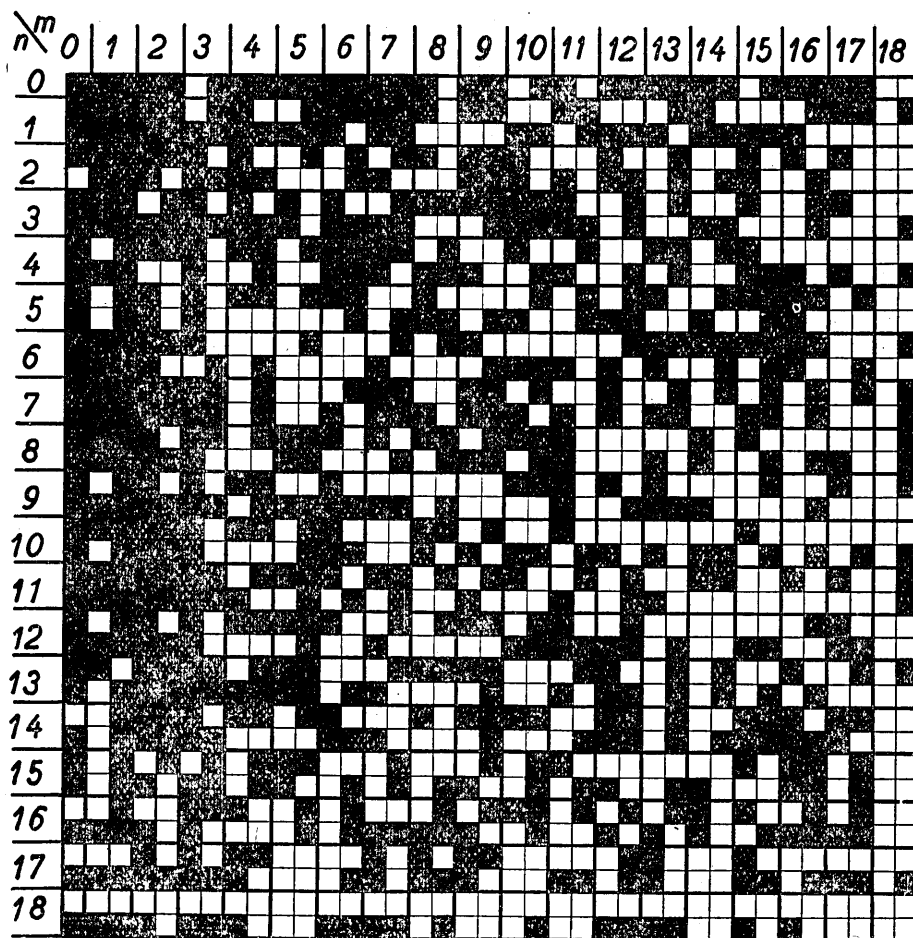


Fig. 3.

they have opposite algebraic signs, then the proper domain of the proper square is made black. In Fig. 3, the black domains clearly predominate in that part where $\sqrt{m^2+n^2}$ is small. It must, however, be borne in mind that, since the area in question is not a square, but a rectangle, m and n are not equivalent; the wave-length of the n -th order harmonics in the y -direction being, in the present case, the same as that of the $2n$ -th order harmonics in the x -direction. Therefore, $\sqrt{m^2+4n^2}$, instead of $\sqrt{m^2+n^2}$, is the measure of the order of the

double Fourier harmonics. Table III gives the total number of pairs, those pairs in which H_{mn} and B_{mn} have opposite algebraic sign and its percentage with respect to the total number, arranged according to successive $\sqrt{m^2 + 4n^2}$.

Table III.

$\sqrt{m^2 + 4n^2}$	Total Number of Pairs	Number of Pairs with Opposite Signs	Percentage
0~1	1	1	100
1~2	2	2	100 } 100
2~3	12	12	100
3~4	6	4	67 } 89
4~5	16	13	81
5~6	14	11	79 } 80
6~7	24	18	75
7~8	18	13	72 } 74
8~9	36	20	56
9~10	18	12	67 } 59
10~11	44	27	61
11~12	26	16	62 } 61
12~13	48	29	60
13~14	34	14	41 } 52
14~15	52	29	56
15~16	38	23	61 } 58
16~17	60	34	57
17~18	50	25	50 } 54
18~19	65	40	62
19~20	30	14	47 } 57
20~21	56	28	50
21~22	34	16	47 } 49
22~23	52	33	63
23~24	28	10	36 } 54
24~25	48	25	52
25~26	30	12	40 } 47
26~27	56	35	63
27~28	28	8	29 } 51
28~29	48	27	56
29~30	24	13	54 } 56
30~31	52	27	52
31~32	30	14	47 } 51
32~33	50	26	52
33~34	22	8	36 } 47
34~35	56	30	54
35~36	20	10	50 } 53
36~37	35	19	54
37~38	16	7	44 } 51
38~39	10	5	50
39~40	6	2	33 } 44
40~41	1	0	0
Total	1296	712	55

It is remarkable that, as the order increases, the percentage decreases very regularly from 100 down to 50 (Fig. 4). This fact

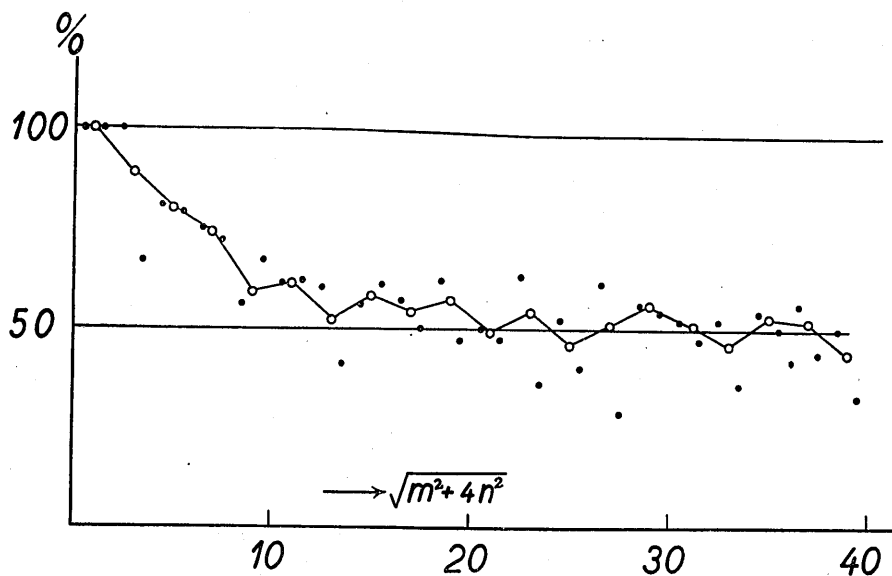


Fig. 4.

suggests that, while the larger topographies are mostly in isostatic equilibrium, the smaller are not, the percentage for these latter being determined by chance.

If we take

$$\sqrt{m^2 + 4n^2} = 20$$

as the threshold value beyond which the percentage is 50, this corresponds to a square with the side

$$\frac{4000 \text{ km}}{\sqrt{20^2/2}} = 290 \text{ km},$$

provided $m=2n$. It is concluded, therefore, that a topography smaller than $145 \text{ km} \times 145 \text{ km}$, which is a quarter of this square, is supported by some mechanism other than isostasy—a conclusion that is important in connection with the problem of local versus regional isostasy.

The next is to determine the thickness of the isostatic earth's crust (in Airy's sense). It was shown that if the thickness is d , then it can be found from the relation

$$-2\pi k^2 \rho H_{m_n} \exp(-\sqrt{m^2 + 4n^2} d) = B_{m_n},$$

where ρ is the density of the crustal material. The most probable

value of d was calculated for pairs up to $\sqrt{m^2+4n^2}=20$ for each order, separately, by using the values of H_{mn} and B_{mn} that were already found. Table IV gives the results of the calculations.

Table IV.

$\sqrt{m^2+4n^2}$	Number of Pairs Used in the Calculations	d (radian)	d (km)
1~2	2	0.103	67.1
2~3	12	0.119	77.6
3~4	4	—	—
4~5	13	0.035	22.8
5~6	11	0.076	49.5
6~7	18	0.046	30.0
7~8	13	0.119	77.6
8~9	20	0.065	42.4
9~10	12	0.043	28.0
10~11	27	0.056	36.5
11~12	16	0.073	47.6
12~13	29	0.046	30.0
13~14	14	0.039	25.4
14~15	29	0.045	29.3
15~16	23	0.042	27.4
16~17	34	0.028	18.3
17~18	25	0.006	3.9
18~19	40	0.008	5.2
19~20	14	0.041	26.7

In Fig. 5, in which d is plotted against $\sqrt{m^2+4n^2}$, there is likely to be a tendency for d to decrease with increase in $\sqrt{m^2+4n^2}$, which tendency, although not very clear owing to scattering of points, suggests that the depth at which the isostatic compensation is completed might depend on the horizontal extent of the topography to be compensated. But, considering the accuracy of

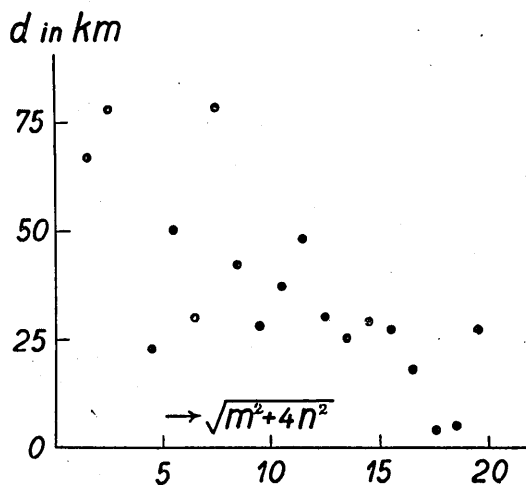


Fig. 5.

the double Fourier coefficients for H and $\Delta g''_o$, much weight cannot be placed on any conclusion derived from small values of H_{mn} and B_{mn} . Selecting those pairs in which

$$H_{mn} > 50 \text{ m}$$

$$B_{mn} > 5 \text{ mgal},$$

we have the following 15 pairs (Table V).

Table V.

$\sqrt{m^2+4n^2}$		H_{mn} (m)	B_{mn} (mgal)	d	Weight
1.00	cos cos	-394	42.1	0.0987	33
1.00	sin cos	611	-64.0	0.1210	78
2.00	cos cos	-138	13.4	0.0962	15
2.00	cos sin	-168	10.1	0.3367	12
2.00	sin cos	-267	25.6	0.0842	55
2.24	cos sin	-161	13.2	0.1630	21
2.24	sin sin	-169	8.9	0.3600	12
2.24	sin cos	-246	25.2	0.0628	62
2.83	sin sin	-180	13.2	0.1682	36
4.00	cos cos	-84	5.3	0.1564	13
4.00	sin cos	-86	7.3	0.0821	20
4.00	cos sin	-59	6.9	0.0025	13
4.47	cos cos	84	-7.3	0.0685	24
4.47	sin cos	99	-11.6	0.0011	46
5.00	sin sin	97	-10.4	0.0191	50

Since

$$B_{mn} = -2\pi k^2 \rho H_{mn} \exp(-\sqrt{m^2+4n^2}d),$$

we have

$$\frac{\Delta B_{mn}}{B_{mn}} = -\frac{\Delta H_{mn}}{H_{mn}} + \sqrt{m^2+4n^2} \Delta d.$$

Therefore $\frac{1}{|\Delta d|^2}$, where

$$\Delta d = \frac{1}{\sqrt{m^2+4n^2}} \sqrt{\left(\frac{\Delta B_{mn}}{B_{mn}}\right)^2 + \left(\frac{\Delta H_{mn}}{H_{mn}}\right)^2},$$

is a measure of the weight to be attributed to each d that was derived from a pair of these H_{mn} and B_{mn} . For

$$\Delta B_{mn} = 5 \text{ mgal}$$

$$\Delta H_{mn} = 50 \text{ m}$$

the weight for each d becomes like that shown in Table V. The weighted mean of d is then

$$\begin{aligned} d &= 0.096 \pm 0.020 \\ &= 61 \pm 13 \text{ km.} \end{aligned}$$

In order to get the thickness of the isostatic earth's crust for zero height, the thickness of the mass that is compensating the average height of 600 m should be subtracted from d . Thus we finally get

$$61 - 5 = 56 \text{ km.}$$

The depth of compensation in Pratt's sense of isostasy, which is twice this value, is consequently 112 km, which agrees very well with the 113.7 km already found by the trial and error method.

3. In the above calculations, m in the x -direction and n in the y -direction were not equivalent, because the distance, which was taken to be 2π , differed for the two directions. From physical considerations, it is more reasonable to take 4000 km in the x -direction to be π and 2000 km in the y -direction to be $\frac{\pi}{2}$, and to express the distribution of

the quantity to be studied by a double Fourier series, with additions of its mirror images, as in Fig. 6.

The series for this case has cos-cos terms only. The coefficients found are shown in Table VI. Although the coefficients H_{mn} and B_{mn} for this case should be the same as $H_{\frac{m}{2}\frac{n}{4}}$ and $B_{\frac{m}{2}\frac{n}{4}}$ in the foregoing case, there are actually small differences between them, which are due to inaccuracies in the practical harmonic analysis.

Out of the total 190 pairs of coefficients of B_{mn} and H_{mn} , 122 (64%) have opposite algebraic signs. The total number of pairs, the number of pairs in which B_{mn} and H_{mn} have opposite signs, and its percentage with respect to the total number are shown in Table VII, according to $\sqrt{m^2+n^2}$, separately. The distribution of pairs in which H_{mn} and B_{mn} have opposite signs, is shown in Fig. 7 on the same scheme as in the previous case. But, since in this case, there are cos-cos terms only, it was not necessary to subdivide a small square determined by m and n into four smaller ones. The decrease in percentage with increase in the order $\sqrt{m^2+n^2}$ is again remarkable

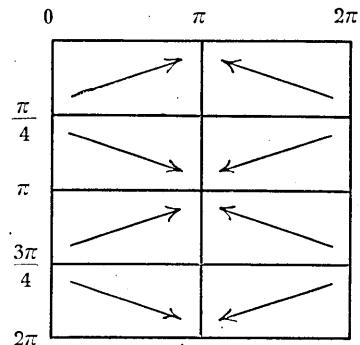


Fig. 6.

Table VI b. B_m in mgal.

$n \backslash m$	0	1	2	3	4	5	6	7	8	9	10	11	12	13	14	15	16	17	18
0	-71.2	-41.6	41.8	54.7	13.9	1.3	4.2	5.8	5.1	1.8	1.7	0.3	-0.2	-1.9	-1.1	-0.5	-0.4	-0.1	-0.1
1																			
2	-9.4	-12.3	18.7	-2.4	13.9	17.7	-0.6	-0.1	-1.1	3.2	2.2	-0.7	1.6	0.6	-0.7	-0.7	-0.4	0.4	-0.6
3																			
4	28.2	17.8	-10.1	-15.4	-2.8	-4.1	-8.6	-8.7	-5.8	2.4	1.4	1.9	-3.1	0.5	0.3	0.2	-0.8	1.0	0.9
5																			
6	-5.7	-7.5	-2.9	6.4	1.4	6.1	4.1	-2.0	1.4	-6.4	0.3	-1.5	1.9	-0.5	-0.1	-1.1	-0.1	-0.3	-0.0
7																			
8	-2.2	-3.6	-4.3	-5.5	-4.5	6.4	3.3	3.6	-0.2	1.0	2.5	1.6	1.7	0.5	0.1	-0.5	1.1	-1.3	-0.2
9																			
10	0.4	-2.4	-4.1	-3.8	-1.2	0.9	0.2	-1.0	2.1	2.0	0.3	2.4	0.9	2.1	1.1	0.9	0.5	0.4	-0.2
11																			
12	1.4	-1.8	0.9	-2.1	-3.2	0.4	-0.3	0.9	1.4	0.5	0.3	-1.1	0.5	-0.7	1.3	0.9	-0.0	-0.7	+0.0
13																			
14	1.2	0.3	-1.0	1.8	-0.3	-2.2	0.5	0.9	-1.3	0.5	-0.1	-0.4	-0.7	0.2	-0.2	-1.1	-0.1	-0.6	0.1
15																			
16	-0.7	-0.3	-0.8	-0.0	2.3	-1.3	0.1	1.1	-0.3	0.4	-0.8	0.1	-0.5	0.2	-0.1	1.0	-0.6	0.6	0.1
17																			
18	-0.2	-0.8	0.4	-0.1	-0.3	-0.1	-1.0	0.1	0.1	1.2	-0.0	0.1	1.1	0.1	-0.5	0.4	0.6	0.3	-0.1

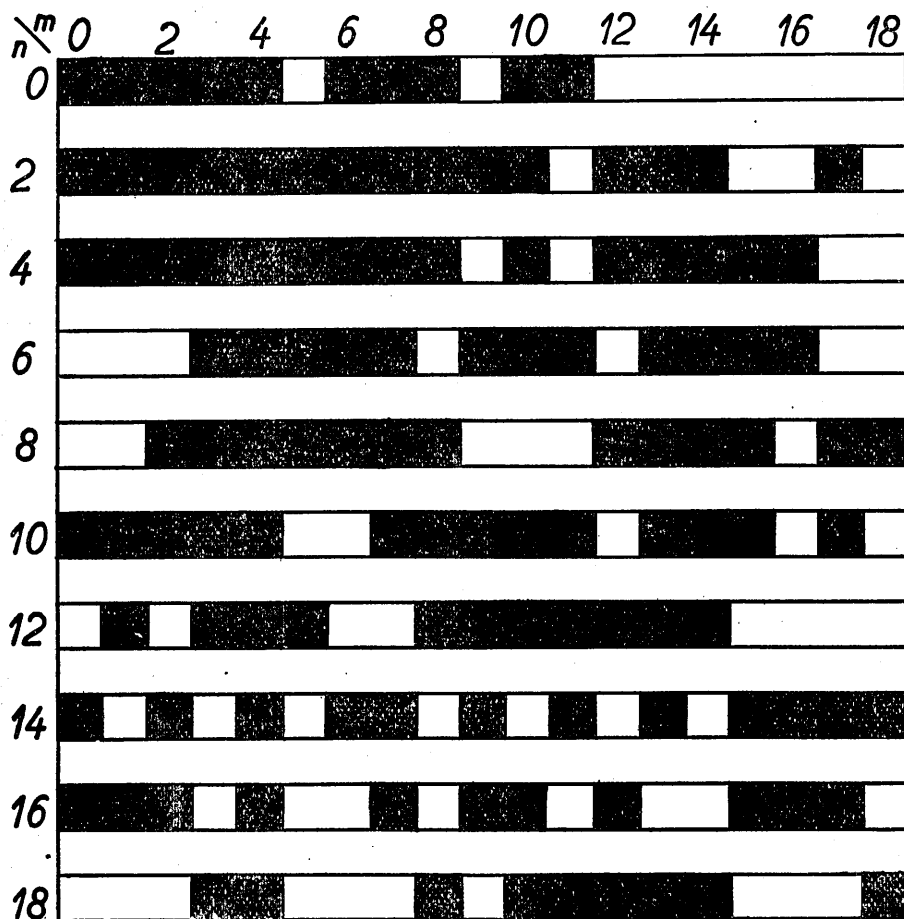


Fig. 7.

Table VII.

$\sqrt{m^2+n^2}$	Total Number of Pairs	Number of Pairs with Opposite Sign	Percentage
0~1	1	1	100
1~2	1	1	100
2~3	4	4	100
3~4	2	2	100
4~5	5	5	100
5~6	4	3	75
6~7	7	4	57
7~8	5	5	100
8~9	10	8	80
9~10	5	3	60

Table VII. (continued)

$\sqrt{m^2+n^2}$	Total Number of Pairs	Number of Pairs with Opposite Signs	Percentage
10~11	12	11	74
11~12	7	3	
12~13	13	8	55
13~14	9	4	
14~15	14	10	71
15~16	10	7	
16~17	16	11	62
17~18	13	7	
18~19	19	7	41
19~20	8	4	
20~21	8	3	50
21~22	6	4	
22~23	5	5	86
23~24	2	1	
24~25	3	0	25
25~26	1	1	
Total	190	122	64

(Fig. 8), although there are large fluctuations owing to scantiness of data. Remembering that $\sqrt{m^2+n^2}=25$ in this case corresponds to $\sqrt{m^2+4n^2}=12.5$ in the foregoing case, the agreement of Figs. 4 and 8 is very satisfactory. For the 122 pairs of B_{mn} and H_{mn} , in which the signs are opposite, the thickness of the isostatic earth's crust d was calculated for each $\sqrt{m^2+n^2}$ separately, according to the relation

$$-2\pi k^2 \rho H_{mn} \exp(-\sqrt{m^2+n^2}d) = B_{mn}$$

with results as shown in Table VIII.

Selecting, as before, those pairs in which

$$H_{mn} > 50 \text{ m}$$

$$B_{mn} > 5 \text{ mgal,}$$

we have the 17 pairs shown in Table IX. The weighted mean of d was found to be 52 ± 4 km.

4. Finally, seeing that both the topography and the Bouguer anomaly in the United States extend, roughly speaking, with but little variation in the N-S direction, our two dimensional method will be used in

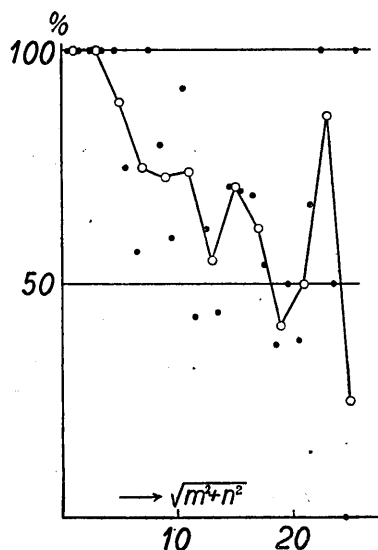


Fig. 8.

Table VIII.

$\sqrt{m^2+n^2}$	d (radian)	d (km)	$\sqrt{m^2+n^2}$	d (radian)	d (km)	$\sqrt{m^2+n^2}$	d (radian)	d (km)
0~1			9~10	0.096	122	18~19	0.049	62
1~2	0.103	128	10~11	0.085	108	19~20	0.019	24
2~3	0.062	79	11~12	0.093	118	20~21	0.100	127
3~4	0.025	32	12~13	0.063	80	21~22	0.066	84
4~5	0.012	15	13~14	0.038	48	22~23	0.017	22
5~6	0.009	11	14~15	0.036	46	23~24	0.003	4
6~7	0.077	98	15~16	0.011	14	24~25	—	—
7~8	0.111	141	16~17	0.038	49	25~26	0.003	4
8~9	0.097	123	17~18	0.038	49			

Table IX.

$\sqrt{m^2+n^2}$	m	n	H_{mn} in m	B_{mn} in mgal	d	Weight
1.00	1	0	408.2	-41.6	0.146	33
2.00	2	0	-359.3	41.8	0.055	128
2.00	0	2	137.3	-9.4	0.273	10
2.24	1	2	162.1	-12.3	0.198	16
2.82	2	2	174.4	-18.7	0.034	52
3.00	3	0	-515.7	54.7	0.035	509
4.00	4	0	-133.6	13.9	0.032	59
4.00	0	4	-245.3	28.2	0.007	219
4.12	1	4	-197.8	17.8	0.065	119
4.47	4	2	-107.8	13.9	—	—
5.00	3	4	156.1	-15.4	0.036	120
5.38	5	2	-146.2	17.7	—	—
6.71	3	6	-54.7	6.4	0.001	31
7.00	7	0	-92.3	5.8	0.090	47
7.21	6	4	59.6	-8.6	—	—
7.81	5	6	-58.5	6.1	0.016	44
8.00	8	0	-72.2	5.1	0.064	44
8.06	7	4	105.1	-8.7	0.044	117
8.94	8	4	66.3	-5.8	0.033	61
10.82	9	6	65.2	-6.4	0.017	98

studying the average E-W profiles of $\Delta g''_0$ and H . The average values of the topography and the Bouguer anomaly are shown in Table X and

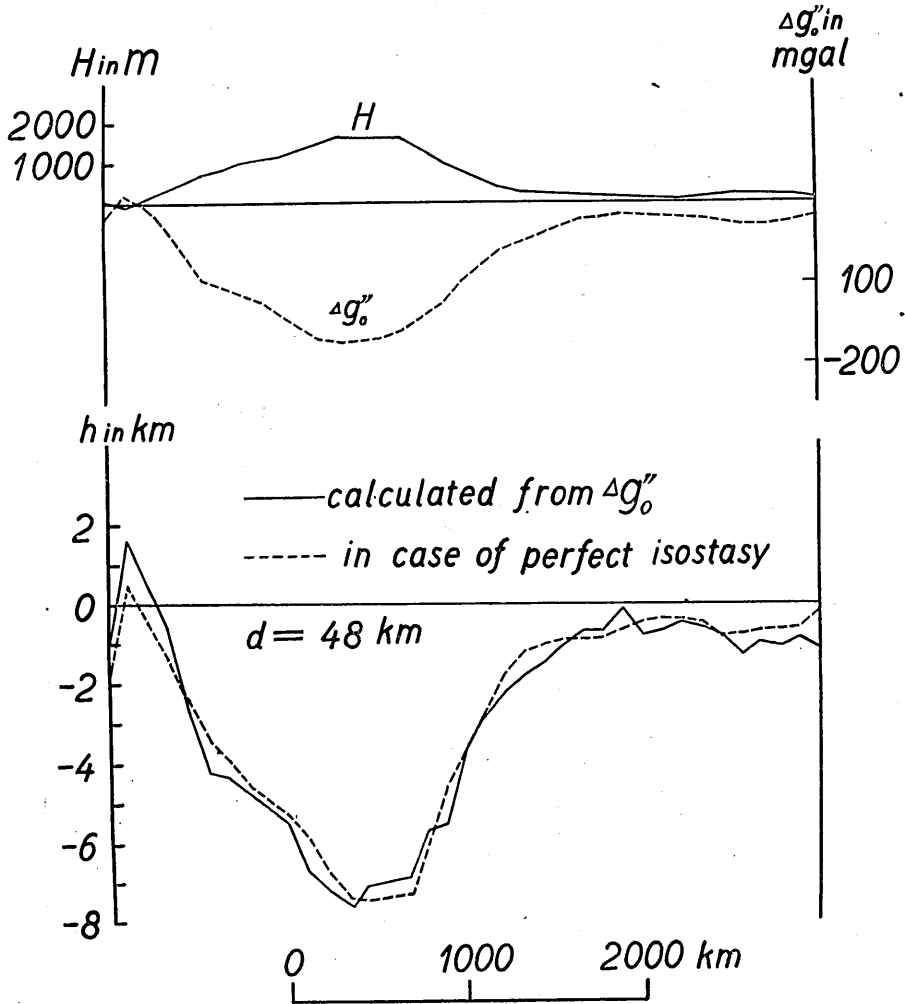


Fig. 9.

in Fig. 9. The whole length of the profile is 4000 km as before. These quantities were analysed into Fourier series like

$$H(x) = \sum_0^{18} H_m \frac{\cos mx}{\sin mx}$$

$$\Delta g''_0(x) = \sum_0^{18} B_m \frac{\cos mx}{\sin mx}.$$

The coefficients H_m and B_m of these series must be equal to H_{m_0} and

Table X.

x	H in m	$\Delta g''_o$ in mgal	x	H in m	$\Delta g''_o$ in mgal	x	H in m	$\Delta g''_o$ in mgal
1	- 91	+ 11	13	1636	-171	25	169	- 20
2	94	0	14	1651	-166	26	129	- 13
3	307	- 27	15	1621	-159	27	103	- 19
4	528	- 64	16	1344	-140	28	89	- 18
5	753	- 96	17	1033	-127	29	80	- 18
6	863	-105	18	811	- 96	30	115	- 19
7	1032	-115	19	593	- 76	31	175	- 23
8	1103	-125	20	379	- 59	32	179	- 28
9	1169	-140	21	263	- 49	33	156	- 29
10	1317	-159	22	215	- 40	34	158	- 28
11	1503	-170	23	206	- 29	35	123	- 25
12	1641	-174	24	197	- 21	36	41	- 17

Table XI.

m	H_m in m		B_m in mgal	
	cos	sin	cos	sin
0	602		-70.9	
1	-394	611	42.1	- 64.0
2	-138	-267	13.4	25.6
3	- 6	43	3.7	2.9
4	- 84	- 86	5.3	7.3
5	- 3	- 28	1.2	5.9
6	1	- 16	- 1.2	6.2
7	2	- 19	- 2.6	0.9
8	- 6	- 11	- 1.5	0.7
9	13	- 31	- 1.1	0.1
10	8	1	- 1.0	0.8
11	- 11	- 11	- 0.1	0.1
12	4	- 8	- 0.3	0.6
13	5	- 10	- 1.0	0.6
14	13	- 8	- 0.2	1.1
15	14	0	- 1.1	- 0.5
16	6	4	- 0.4	- 0.3
17	8	- 2	- 1.4	0.1
18	3		0.2	

B_{m_0} of the double Fourier series that were given in Tables I and II. Out of the whole 36 pairs of B_m and H_m , 31 pairs have opposite algebraic signs, indicating that isostasy holds nearly perfectly for this

average profile. The weighted mean of the thickness of the isostatic earth's crust determined from those pairs in which

$$H_m > 50 \text{ m}$$

$$B_m > 5 \text{ mgal}$$

is $67 \pm 2 \text{ km}$ (Table XII).

Table XII.

m	H_m	B_m	d	Weight
1	-394	42.1	0.0987	33
1	611	-64.0	0.1210	78
2	-138	13.4	0.0962	15
2	-267	25.6	0.0842	55
4	-84	5.3	0.1564	13
4	-86	7.3	0.0821	20

By putting d to be 0.074 (48 km), for instance, it is possible to find the mass at that depth that will cause the observed Bouguer anomalies. This can be done by synthesizing the series

$$\rho(x) = \frac{1}{2\pi k^2} \sum B_m \exp(md) \frac{\cos mx}{\sin mx}.$$

If this mass is interpreted as due to the undulation of the boundary surface between the crustal and the denser subcrustal materials, the relief of the boundary is given by

$$h(x) = \rho(x) / \Delta\rho.$$

If we take $\Delta\rho = 0.6$, we get the values shown in Table XIII and in Fig. 9. In the table, the relief h' of the same boundary for that case in which isostasy is perfect is also shown for the sake of comparison. The agreement of h and h' is surprisingly good; the difference in the two reliefs being mostly less than 1 km.

Table XIII.

x	h in km	h' in km	$h-h'$ in km	x	h in km	h' in km	$h-h'$ in km
0	-1.0	-1.9	+0.9	4	-2.7	-2.4	-0.3
1	1.6	0.4	+1.2	5	-4.2	-3.4	-0.8
2	0.5	-0.4	+0.9	6	-4.3	-3.9	-0.4
3	-0.6	-1.4	+0.8	7	-4.7	-4.6	-0.1

Table XIII. (continued.)

x	h in km	h' in km	$h-h'$ in km	x	h in km	h' in km	$h-h'$ in km
8	-5.1	-5.0	-0.1	23	-1.0	-0.9	-0.1
9	-5.5	-5.3	-0.2	24	-0.7	-0.9	+0.2
10	-6.7	-5.9	-0.8	25	-0.7	-0.8	+0.1
11	-7.2	-6.8	-0.4	26	-0.1	-0.6	+0.5
12	-7.5	-7.4	-0.1	27	-0.8	-0.5	-0.3
13	-7.0	-7.4	+0.4	28	-0.7	-0.4	-0.3
14	-6.9	-7.4	+0.5	29	-0.5	-0.4	-0.1
15	-6.8	-7.3	+0.5	30	-0.6	-0.5	-0.1
16	-5.7	-6.0	+0.3	31	-0.8	-0.8	0
17	-5.5	-4.6	-0.9	32	-1.3	-0.8	-0.5
18	-3.6	-3.6	0	33	-1.0	-0.7	-0.3
19	-2.8	-2.7	-0.1	34	-1.1	-0.7	-0.4
20	-2.2	-1.7	-0.5	35	-0.9	-0.6	-0.3
21	-1.8	-1.2	-0.6	36	-1.0	-0.2	-0.8
22	-1.5	-1.0	-0.5				

In conclusion, the writers wish to express their thanks to Professor Sakuhei Fujiwhara for his kindly interest in the present study.

24. 重力異常と地下構造との關係 (IV)

地震研究所 坪 井 忠 二
 地震學教室 { 金 子 徹 一
 矢 橋 德 太 郎

北米合衆國に於ける重力異常と地形との關係を吟味し次の結果を得た。

- 1) 北米合衆國では均衡が非常によく成立つて居る。
- 2) Airy 流の地殻の厚さは

$$47 \pm 4 \text{ km.}$$

である。

- 3) 地方的補償の限界は一邊 145 km. である。